

Theoretical Study of Electromagnetic Scattering by Metal Nanoparticles

Samantha Bruzzone,* Marco Malvaldi, Giovanni P. Arrighini, and Carla Guidotti

Dipartimento di Chimica e Chimica Industriale, Università di Pisa, Via Risorgimento 35, 56100 Pisa, Italy

Received: October 6, 2004; In Final Form: December 20, 2004

Progress in near-field optical spectroscopy research on metal nanoparticles demands a better understanding of the role of particle–particle and tip–sample interactions. In this perspective, we investigate theoretically, at a very moderate level of sophistication, the optical behavior of simple silver nanoparticle aggregates, in terms of a formalism involving a multipolar expansion of the fields involved, along with a simplified model for the optical behavior of nanostructures previously developed. In particular, the tip–sample interaction is taken into account roughly, treating the tip as an additional, single particle, characterized by proper dielectric behavior.

I. Introduction

Plenty of theoretical and experimental work in the past decade has been directed to the study of the electromagnetic (em) response of metallic nanoparticles exposed to UV–visible radiation.^{1–5} In most cases, the attention has been addressed to the em far-field response; but it is uncontroversial that there is not yet complete understanding of how, through the interplay of fundamental interactions, near-field effects in proximity to the particle surface manifest themselves.⁶ Direct knowledge of such interactions is fundamental to correctly address optical phenomena appearing at the nanometric scale. To get a deeper insight on this matter and to overcome the spatial resolution limitation of traditional spectroscopy, scanning near-field optical microscopic (SNOM) techniques were developed in (and have been increasingly used since) the mid-1980s.^{7–8} Within years, the technical setup of the scanning near-field devices has offered new opportunities, for example, detecting evanescent fields in guiding structures,⁹ imaging of nanopatterned structures, and excited localized plasmons over a metallic surface.¹⁰ In addition, SNOM analysis performed on nanometric samples has evidenced phenomena of em field localization; such behavior, considering the current trends toward miniaturization of optical devices, could be exploited for different useful applications.

There is broad consensus that SNOM techniques at present provide a unique method to penetrate the complexity of matter–radiation interactions at nanometric scales, without mentioning that the possibility of measuring field intensities near surfaces could, in principle, be useful to quantitatively investigate surface-enhanced spectroscopies, such as SERS. The full understanding, from a theoretical point of view, of the mechanism ruling the SNOM measurements surely would be of great help to better interpret the results coming from experiments and to develop further advances in such kind of analysis.

We limit ourselves to briefly recall that SNOM is a technique involving basically a sharp nanoscopic probe, able to scan a given surface at a subwavelength distance. In a commonly used instrumental setting, the sample lies on a glass prism, which enables one to shine light in total internal reflection. The nanometer-size tip scanning the surface then frustrates the total

reflection, to send light to the detector.¹¹ The amplitude of the scattered light is related to the amplitude of the near-field that locally illuminates the tip. The mechanism by which some components of the evanescent illuminating field can be transformed into propagating field components that carry information about the sample are at the core of image formation in SNOM.¹² In particular, frequently discussed (and remaining still an open problem) is the role played by interactions between the sample and the tip.¹³

The present work proposes itself as a plain contribution to this discussion. By relying on a previously developed model of em extinction and scattering by aggregates of spherical particles (see *infra*), we attain a coarse-grained representation of an apertureless near-field optical microscopy. The aim of the study is to obtain, by implementing relevant numerical calculations, simulated near-field microscopy images. The simulations performed account explicitly for the tip probe–sample interaction. This kind of calculation could be of value in both interpreting experimental images (which are sometimes not trivial to be interpreted) and better understanding the role of fundamental phenomena, in the broader radiation–metal surface interaction context.

The whole problem of the near-field optical response can be fully framed in the general formulation of em scattering by particle aggregates. Light scattering and absorption (i.e., extinction) by arbitrarily shaped particles have been the subject of numerous studies in optics and, more generally, in electrodynamics. Optical effects associated with cluster aggregates are well-known for noble metal particles. A significant feature of such effects is documented by the splitting of the surface plasmon resonance of the isolated (spherical) particle into new modes as a consequence of the em coupling among the particles, with interesting effects concerning, for instance, the color assumed by colloidal emulsions, caused by changes in their absorption spectra. In line with preceding considerations, however, our emphasis in the present paper is placed essentially on the general role of the interactions between sample particles and between particles and tip probe in building up SNOM theoretical models.

In section II the system studied and the model utilized will be briefly outlined, whereas numerical results and discussion are addressed in sections III and IV.

* Corresponding author: tel +39-50-2219294; fax +39-050-2219260; e-mail sama@cci.unipi.it.

II. Model and Calculations

In this work we present some numerical results concerning em scattering by small aggregates, taking due allowance for the electromagnetic coupling among all particles. The system considered to a greater extent involves $N = 5$ identical, nanosized Ag particles (sample), lying in the xy plane, and a single, larger particle (radius $R_{\text{tip}} = 20$ nm), characterized by appropriate dielectric properties (tip probe). For simplicity, it is assumed that both sample and tip probe are embedded in a homogeneous medium (vacuum). The dielectric behavior of the metal particles takes approximately into account effects related to their dimensions (size effects). An incident plane em wave (wavelength λ) is scattered and partially absorbed by each particle. As a given particle (say i) is in the neighborhood of the other $N - 1$ particles, all scattered waves by these $N - 1$ particles will contribute obviously to the em field felt by the specific particle i considered. The center of the particle probe scanning the sample plane (x, y) belongs to the plane $z = z_{\text{tip}}$. Different values of $h = z_{\text{tip}} - R_{\text{tip}}$ have been used in distinct simulations (for a clear view of the topological arrangement of the particles involved, see also Figures 1 and 2). For any tip position, we calculate the scattered intensity $|\vec{E}_{\text{sc}}|^2$ at the point individuated by the same (x, y) values of the tip center and z -coordinate corresponding to $z = h = z_{\text{tip}} - R_{\text{tip}}$ [so that (x, y, z) refers to the lower surface of the tip].

The calculation of $|\vec{E}_{\text{sc}}|^2$ have been carried out following the very general treatment elaborated by Gérardy and Ausloos,¹⁴ successively reconsidered also by others.^{15,16} We shall limit ourselves to recall briefly the main lines of the approach implemented in our computational code, referring one for details to the original sources quoted. Yet, before, a few comments about the problem of the SNOM-image interpretation are appropriate.

In this work, we assume that the signal measured in SNOM experiments is directly correlated with the near-field em intensity illuminating the tip. Our assumption is supported both theoretically by reviews by Greffet and Carminati¹⁸ and Girard and Dereux,¹⁹ where our intuitive identification is discussed and justified, and experimentally by recent works.^{11,17} Other (physically sound) possible choices, however, must be recognized; in other theoretical works, for instance, the SNOM images at different tip localizations have been correlated with scattering section data.

In its most general formulation, the theoretical study of the classical em scattering from an aggregate of particles with arbitrary topology is not a trivial task, even in the case of spherical particles. The treatment, a generalization of the Mie theory,^{20,21} starts from the solution of Maxwell's equations, with standard boundary conditions at the surface of each particle for the fields, which are expanded in terms of vector spherical harmonics.^{22,23} By use of vector addition theorems and spherical harmonic transformation properties to represent the fields scattered by the particle j in terms of an expansion in vector spherical harmonics centered at the particle i , an equation set for the expansion coefficients of the em wave scattered by the particle i is derived. Starting from the knowledge of scattering data relative to a single, isolated sphere, for the transverse magnetic (TM) and transverse electric (TE) modes associated with the various orders of multipole, whose expressions are well-known,^{20,21} the equation set can be solved. As these coefficients depend on the dielectric function of the particle, the desired expansion coefficients will reflect the dielectric behavior of the particles constituting the aggregate. The dielectric function of the metal particles involved has been approximated by us,

Particle	1	2	3	4	5
X(nm)	25	25	25	10	40
Y(nm)	25	10	40	25	25

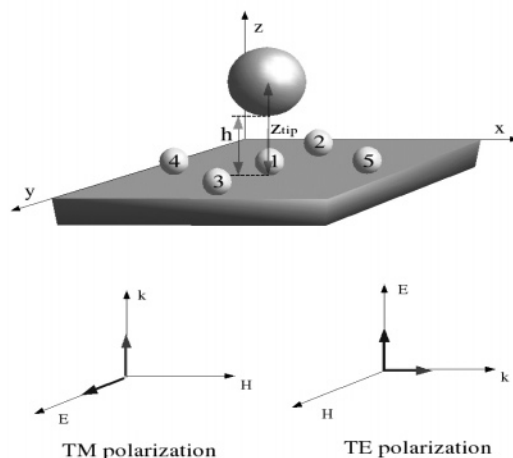


Figure 1. Schematic representation of the simulated experimental setup. The top panel reports the coordinates of the metal particles in reduced length units ($=4$ nm). The tip probe spans the (x, y) plane, at a fixed height z_{tip} along the z -axis. Note that locations, particle and tip probe radii are not in scale. The spatial arrangement of the fields, in the polarizations adopted, is represented in the lower panel.

relying on a simple model extensively treated by some of us in earlier works,^{25,26} based on the behavior of a noninteracting electron gas confined in a box, enabling us to take into account quantum size effects in a simple yet efficient way. The “tip” dielectric function has been, instead, assumed constant, of value $\epsilon_{\text{tip}} = 1.44$.² We remark that this value of ϵ_{tip} might be smaller than the effective one,² but such an occurrence should not be judged as detrimental, considering the nature of this paper.

As already remarked,¹⁵ involved multipole–multipole coupling effects decrease with increasing interparticle i, j distance. In particular, as distances become greater than 5 times the sum of i, j particles radii, these effects become almost completely negligible. We will return to this issue later, discussing the absorption spectra of a few SNOM particle aggregates considered in the following. On the basis of the theoretical approach¹⁴ described above, the absorption efficiency $Q_{\text{abs}}(\omega)$ of an aggregate of particles can be calculated in a simple way, starting from the knowledge of the same expansion coefficients at different frequencies.

III. Results and Discussion

The results discussed in this paper refer to small planar clusters constituted by a small number (N) of identical, spherical Ag particles (radius R), lying in the $z = 0$ plane. The geometrical characterization of the aggregates considered is provided in Figure 1 (five particles packed in a cross-shaped structure) and in Figure 2 (four particles, structure obtained from the preceding one by removing the central particle), respectively. For reasons of graphical convenience, a length unit of 4 nm has been adopted. In each case, as already stated, the center of the probe

Particle	1	2	3	4
X(nm)	10	10	0	20
Y(nm)	0	20	10	10

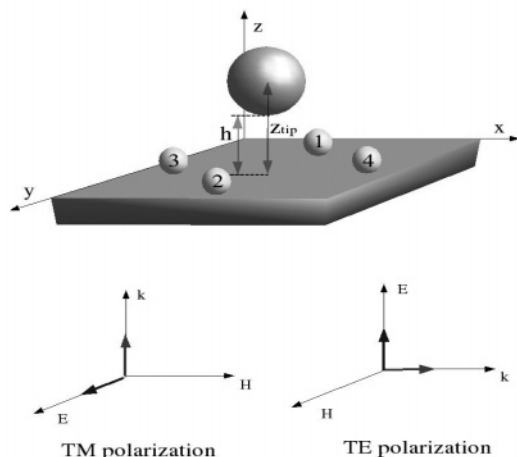


Figure 2. Schematic representation of the experimental setup simulated in Figure 8b (see also caption for Figure 1).

particle explores through successive moves the plane $z_{\text{tip}} = R_{\text{tip}} + h = \text{const}$ parallel to the $z = 0$ one, sampling a total of 51×51 pairs of (x, y) values (scanned by 4 nm steps).

In Figure 3 the absorption efficiency Q_{abs}/N (normalized with respect to the number of particles) is plotted, as a function of the incident wavelength, for two samples of five Ag particles, arranged as in Figure 1, without the presence of the particle simulating the tip probe. Each panel reports the behavior of two different samples, constituted by particles of radius 5 nm (—) and 25 nm (---). Figure 3a refers to the case of an incident em wave propagating along the y axis and electric field oriented along the z axis (TE polarization), while Figure 3b is relative to an incident em wave propagating along the z axis and electric field along the x axis (TM polarization). The inspection of this figure leads one to easily conclude that there are not appreciable interactions in the sample constituted by smaller particles. For different polarizations of the incident field, in fact, the absorption does not change and remains identical to that of a single isolated particle (solid lines in Figure 3). For particles of radius 25 nm, on the contrary, splitting of the surface plasmon is observed, in accordance with the expectation¹⁵ (when the incident wave is propagating parallel to the y axis), a behavior clearly due to electromagnetic coupling between the different particles, which in turn is able to discriminate the longitudinal plasmon from the transversal one, even in the case of spherical particle aggregates (dashed lines in Figure 3). When the electric field of the incident em wave enters perpendicularly the x, y plane, all the particles find themselves in a similar situation with respect to the field and the absorption maximum is not split, resulting in a peak more intense than that produced by 5 nm particles and essentially located at the same wavelength.

We can conclude, therefore, that for the situation involving particles of radius 5 nm, with interparticle separations larger than 5 times their own diameter, the interactions between sample particles will not affect appreciably the scattering behavior, while

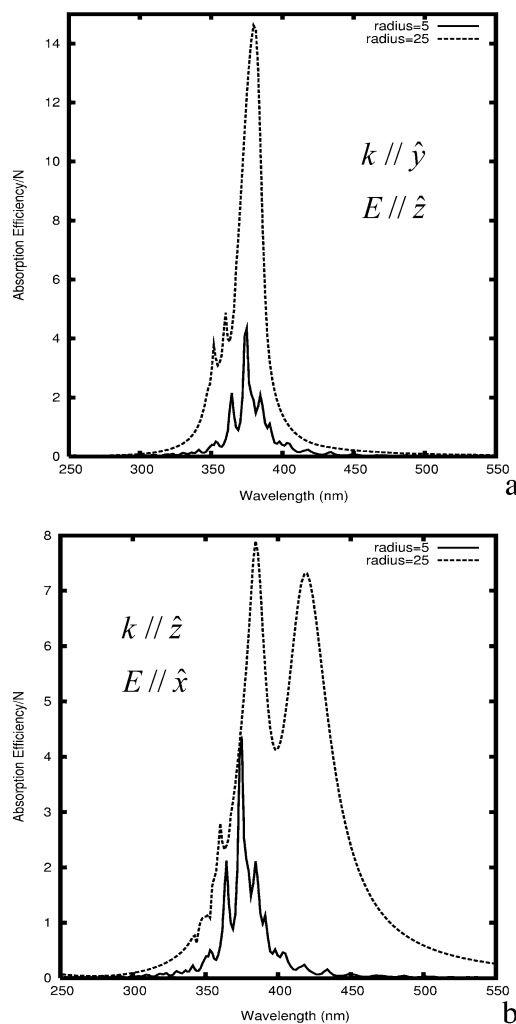


Figure 3. Absorption efficiency Q_{abs} vs optical wavelength for clusters constituted by five Ag particles, with radius 5 nm (—) or 25 nm (---), arranged as in Figure 1 with (a) TE polarization of the incident field or (b) TM polarization of the incident field.

the effects related to the presence of the tip probe particle will be important.

Figure 4 provides examples of calculated three-dimensional maps of the scattered intensity $|\vec{E}_{\text{sc}}|^2$ for a cluster constituted by five Ag particles arranged as in Figure 1, with $R = 5$ nm and different values of the parameters z_{tip} and h . Figure 4a corresponds to a tip simulated by a glassy sphere ($R_{\text{tip}} = 20$ nm), located at $z_{\text{tip}} = 25$ nm, a distance enabling contact with the sample during the tip scanning ($h = 5$ nm). In Figure 4b the probe height rises to $z_{\text{tip}} = 30$ nm ($h = 10$ nm), while the case described by Figure 4c is peculiar, being relative to a (limit) situation characterized by the absence of the probe. The field amplitude is evaluated at $h = 5$ nm, the same height used for the calculation reported in Figure 4a, with the direction of propagation of the incident light along the y -axis and electric field along the z -axis (TE polarization). The purpose is clearly to explore, within this model, a hypothetical case where the tip is not involved in the scattering process, so as to gain some appreciation of the interaction effects existing between metal particles and sphere mimicking the tip. At the chosen wavelength of the incident light ($\lambda = 415.4$ nm), an isolated Ag nanoparticle exhibits strong surface plasmon absorption,¹¹ with associated appreciable effects of local field enhancement.²⁷

The position of each particle is clearly revealed by the field distribution in the xy plane. In Figure 4a, strong localization of

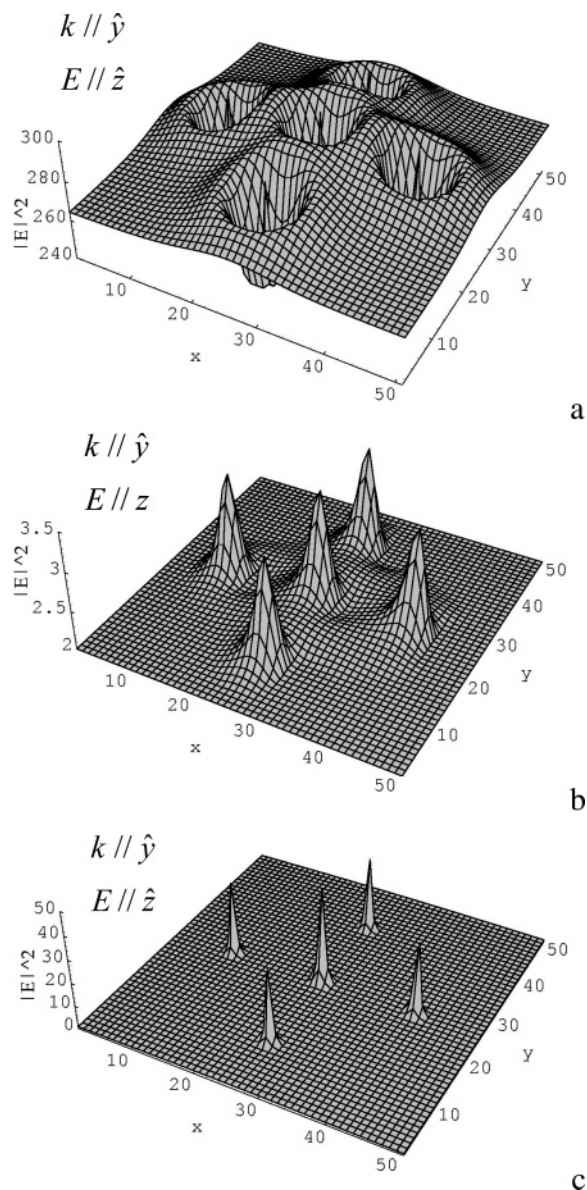


Figure 4. $|\vec{E}_{\text{sca}}(\vec{r})|^2$ plot for different (x, y) positions of the tip probe ($R_{\text{tip}} = 20$ nm) scanning the plane at height $h = z_{\text{tip}} - R_{\text{tip}}$, for a cluster constituted by five Ag particles (radius $R = 5$ nm, coordinates as in the top panel of Figure 1. Incident light propagating along the y -axis, with electric field polarized along the z -axis (TE polarization). (a) $h = 5$ nm; (b) $h = 10$ nm; (c) no tip present, $h = 5$ nm.

the scattered field amplitude around the single particles is observed, along with the presence of a local maximum positioned at the contact point between sample and particle-tip probe, a consequence of the localized surface plasmon resonance and the enhancement of the near-field amplitude parallel to the electric field polarization. The scattered-field pattern around the particles can be explained by the combination of two concomitant effects, the near-field enhancement in the proximity of the particle surface and the destructive interference due to the presence of the probe particle. This interference effect vanishes at the points where contact between sample particles and probe occurs and the distance between their surfaces vanishes. In Figure 4b, the increased separation h leads to disappearance of the destructive interference effects between the fields scattered by the single metal particles and the tip probe, with permanence of a flat background, roughly conforming to the aggregate shape. Figure 4c exhibits the presence of a strongly narrowed and

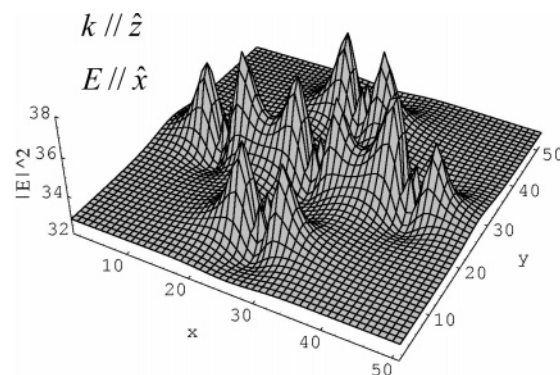
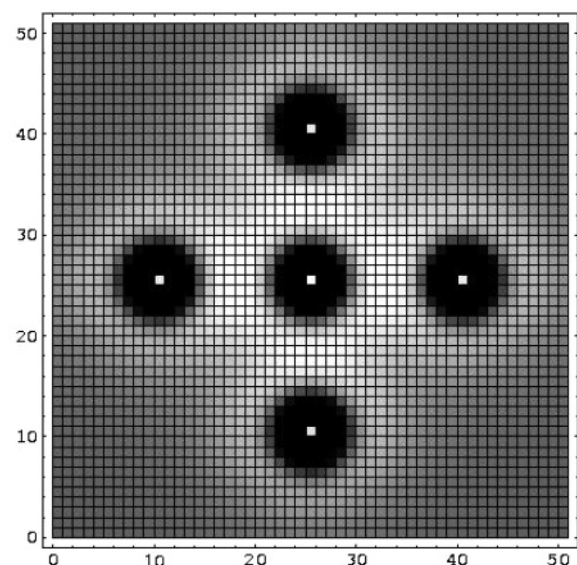


Figure 5. $|\vec{E}_{\text{sca}}(\vec{r})|^2$ plot for different (x, y) positions of the tip probe ($R_{\text{tip}} = 20$ nm) scanning the plane at height $h = 5$ nm, for a cluster constituted by five Ag particles (radius $R = 5$ nm, coordinates as in the top panel of Figure 1. Incident light propagating along the z -axis, with electric field being x -polarized (TM polarization).

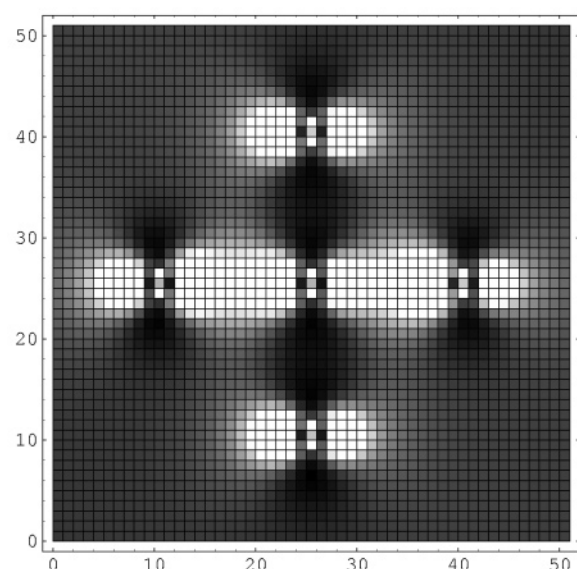
enhanced signal, confirming the previous remark on the interference between scattered fields from tip and metal particles.

In Figure 5, we reconsider the cluster viewed in Figure 4a, in the same topology, the only difference being that here the electric field is oriented along the x -direction, with direction of propagation of the incident light along the z -axis (TM polarization). The three-dimensional map now exhibits an indented structure. In particular, the comparison with Figure 4a evidences that the “holes” around each particle are replaced by several peaks. The signal localization now appears much less sharp, particularly along the x -axis. The peculiar structure observed for the scattering profile can be explained as due to localized surface-plasmon resonance effects, which lead to strong field enhancement only in the same direction of polarization of the electric field (here the direction \hat{x}). As already pointed out, this occurrence can be observed also in Figure 4a, as well as in Figure 4c, where the high-intensity field is along the z direction. A particularly clear illustration of these observations is provided by the inspection of Figure 6, where projections on the xy plane of the three-dimensional maps of Figures 4a and 5 are reported.

To investigate the role of the interactions between sample particles in the framework of the present model, a few additional calculations have been performed on clusters constituted by larger Ag particles, separated by distances equivalent to or smaller than those reported in Figure 1. Figure 7 illustrates the behavior of $|\vec{E}_{\text{sc}}|^2$ for the five Ag-nanoparticle cluster considered previously. The geometrical characterization of the aggregate is again that reported in Figure 1, the essential difference to point out being the radius of the metal particles ($R = 25$ nm), 5 times that of the particles considered in Figures 4 and 5. Size and nature of the sphere probe are unchanged: $z_{\text{tip}} = 50$ nm, while the value of the parameter h has been raised to $h = 30$ nm. The orientation of the incident em field replicates that of Figure 4. A comparison with the map of Figure 4b suggests itself as particularly significant, because in both figures the distance surface-particle-tip and surface-particle-sample along z is 5 nm. Since the calculations underlying Figure 7 refer to particles of larger size compared to those considered in Figure 4, on the basis of Mie theory it is straightforward to expect enhancement of the scattered-field amplitude when passing from the situation analyzed in Figure 4b to the one of Figure 7. It is not yet clear to us, however, whether the effective enhancement (of almost 1 order of magnitude) is related only to the size of the single particles or if a significant role must be recognized for the interactions between particles (more precisely, between their plasmonic modes). As a matter of fact, the increased size of the particles implies a smaller distance between their surfaces,



a $k // \hat{y}$ $E // \hat{z}$



b $k // \hat{z}$ $E // \hat{x}$

Figure 6. Projection on the (xy) plane of the quantity plotted in Figures 1 and 2. (a) Case corresponding to Figure 1a (TE polarization); (b) case corresponding to Figure 2 (TM polarization).

with consequent enhanced coupling between fields scattered by the single particles. Keeping this in mind, the interpretation of the $|\vec{E}_{sc}|^2$ maps reported in Figures 4b and 6 should take into account collective enhancement effects of the scattering efficiency²⁸ in the second case. Anyway, the most evident effect introduced by the presence of interactions between the sample particles is perhaps the influence on the central particle, whose signal now is almost completely erased. This feature, obviously unexplained in terms of single-particle scattering, provides clear, qualitative evidence that interparticle interactions can affect strongly the near-field scattering from aggregates, even if a quantitative estimate is difficult. A more systematic study of the role of this coupling as a function of particle distances, dimensions, wavelength, and polarization of the incident light deserves a more focused discussion, that will be presented in a forthcoming paper.

The last figure reported (Figure 8) refers to a planar cluster involving only four Ag particles (radius $R = 25$ nm), obtained

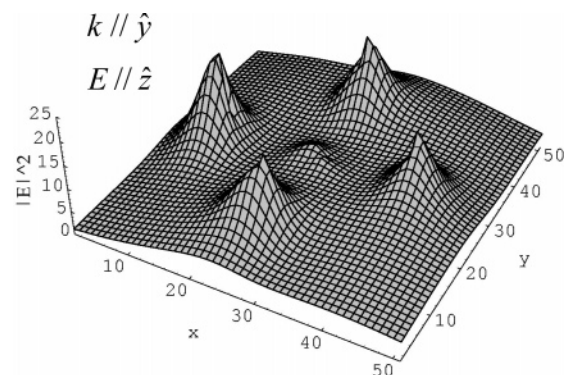
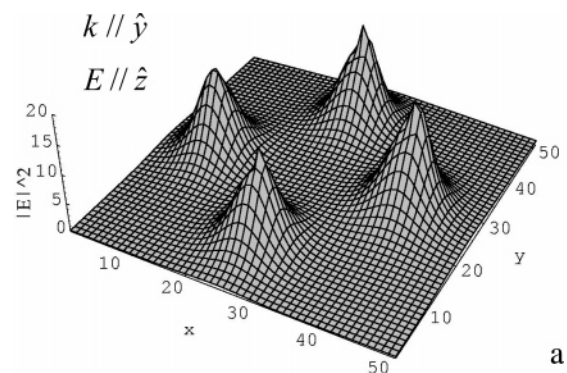
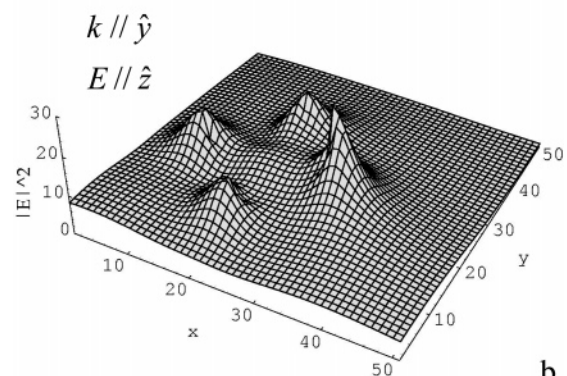


Figure 7. $|\vec{E}_{sca}(\vec{r})|^2$ plot for different (x, y) positions of the tip probe ($R_{tip} = 20$ nm) scanning the plane at height $h = 30$ nm for a cluster constituted by five Ag particles (radius $R = 25$ nm, coordinates as in the top panel of Figure 1. Incident light propagating along the y -axis, with electric field z -polarized (TE polarization).



a



b

Figure 8. $|\vec{E}_{sca}(\vec{r})|^2$ plot for different (x, y) positions of the tip probe ($R_{tip} = 20$ nm) scanning the plane at height $h = 30$ nm, for a cluster constituted by four Ag particles (radius $R = 25$ nm). Incident light propagating along the y -axis, with electric field z -polarized (TE polarization). (a) Metal-particle coordinates as reported in the top panel of Figure 1; (b) metal-particle coordinates as reported in the top panel of Figure 2.

from the larger one by removing the central particle. The nanoparticles are illuminated by light in TE polarization. The $|\vec{E}_{sc}|^2$ results mapped in Figure 8a refer to a particle array whose coordinates are again those reported in Figure 1 (only particles 2–5), while the geometry considered in Figure 8b is that displayed in Figure 2. The different interaction pattern created by removal of the central particle from the larger cluster results in a different relative intensity of the peaks centered on the remaining particles. However, the different coupling between the particles and between particles and tip probe, which are sufficient to modify the peak intensities, is not strong enough to generate light localization in the central zone, as observed for other systems.¹⁷ We can suggest that the particles are

probably still too far, with respect to their dimensions, to give rise to efficient interparticle coupling. Indeed, if the cluster particles are closer (case of Figure 8b), some slight, but detectable, light localization appears at the center of the aggregate, a presence that can eventually be considered sufficient to create artifacts able to lower the quality of the image resolution.

IV. Conclusion

Summarizing, through an acceptable low-cost computational approach we have succeeded in obtaining some qualitative conclusions of possible significance in analyzing near-field scattering phenomena. Starting from a classical electromagnetic scattering picture involving simple cluster models, the presence and influence of interactions between the particles have been studied for a few planar topologies, adopting a simplified quantum-mechanical description for the dielectric function of the metal particles involved. If we accept the oversimplified simulation that the tip probe is representable by a spherical particle, the role of the scanning tip probe role in SNOM becomes roughly analogous to the effects due to the presence of an additional particle at a fixed height z_{tip} . Although the z_{tip} values considered in this paper are purely indicative, theoretical investigations concerning the dependence of the $|\vec{E}_{\text{sc}}|^2$ signal on the h parameter can lead to interesting speculations, as suggested by recent experimental work.¹¹

Acknowledgment. We are indebted to CNR (Progetto Finalizzato MSTA II) and Istituto Nazionale di Fisica della Materia for financial support.

References and Notes

- (1) Serra, L.; Rubio, A. Z. *Phys. D* **1997**, *40*, 262.
- (2) Link, S.; El-Sayed, M. A. *J. Phys. Chem. B* **1999**, *103*, 8410.

- (3) Prodan, E.; Nordlander, P.; Halas, N. J. *Nano Lett.* **2003**, *3*, 1411.
- (4) Pacheco, J. M.; Ekardt, W. P. Z. *Phys. B* **1997**, *103*, 327.
- (5) Palpant, B.; Prével, B.; Lermé, J.; Cottancin, E.; Pellarin, M.; Treilleux, M.; Perez, A.; Vialle, J. L.; Broyer, M. *Phys. Rev. B* **1998**, *57*, 1963.
- (6) Messinger, B. J.; von Raben, K. U.; Chang, R. K.; Barber, P. W. *Phys. Rev. B* **1981**, *24*, 649.
- (7) Pohl, D. W.; Denk, W.; Lanz, M. *Appl. Phys. Lett.* **1984**, *44*, 651.
- (8) Betzig, E.; Harootunian, A.; Lewis, A.; Isaacson, M. *Appl. Opt.* **1986**, *25*, 1890.
- (9) Choo, A. G.; et al. *Appl. Phys. Lett.* **1994**, *65*, 947.
- (10) Dawson, P.; de Fornel, F.; Goudonnet, J. P. *Phys. Rev. Lett.* **1994**, *72*, 2927.
- (11) Wurtz, G. A.; Hranisavljevic, J.; Wiederrecht, G. *Nano Lett.* **2003**, *3*, 1511.
- (12) Girard, C.; Joachim, C.; Gauthier, S. *Rep. Prog. Phys.* **2000**, *63*, 893.
- (13) Dereux, A.; Girard, C.; Weeber, J. C. *J. Chem. Phys.* **2000**, *112*, 7775.
- (14) Gérardy, J. M.; Ausloos, M. *Phys. Rev. B* **1982**, *25*, 4204.
- (15) Quinten, M.; Kreibig, U. *Appl. Opt.* **1993**, *32*, 6173.
- (16) Quinten, M. *Appl. Phys.* **1998**, *67*, 101.
- (17) Peyrade, D.; Quidant, R.; Weeber, J.-C.; Dereux, A.; Léveque, G.; Girard, C.; Chen, Y. *Europhys. Lett.* **2001**, *56*, 517.
- (18) Greffet, J.-J.; Carminati, R. *Prog. Surf. Sci.* **1997**, *56*, 133.
- (19) Girard, C.; Dereux, A. *Rep. Prog. Phys.* **1996**, *59*, 657.
- (20) Bohren, C. F.; Huffman, D. R. *Absorption and Scattering of Light by Small Particles*; Wiley: New York, 1983.
- (21) Van de Hulst, H. C. *Light Scattering by Small Particles*; Dover: New York, 1981.
- (22) Stratton, J. A. *Electromagnetic Theory*; McGraw-Hill: New York, 1941.
- (23) Jackson, J. D. *Classical Electrodynamics*; John Wiley & Sons: New York, 1962.
- (24) Ohfuti, Y.; Amanai, T. *J. Lumin.* **2000**, *87–89*, 960.
- (25) Bruzzone, S.; Arrighini, G. P.; Guidotti, C. *Chem. Phys.* **2003**, *291*, 125.
- (26) Bruzzone, S.; Malvaldi, M.; Arrighini, G. P.; Guidotti, C. *J. Phys. Chem. B* **2004**, *108*, 10853.
- (27) Wurtz, G. A.; Dimitrijevic, N. M.; Wiederrecht, G. P. *Jpn. J. Appl. Phys.* **2002**, *41*, L351.
- (28) Krenn, J. R.; Weeber, J. C.; Dereux, A.; Bourillot, E.; Goudonnet, J. P.; Schider, B.; Leitner, A.; Aussenegg, F. R.; Girard, C. *Phys. Rev. B* **1999**, *60*, 5029.